第 19 卷 第 1 期
2005 年 03 月

实 验 流 体 力 学
Journal of Experiments in Fluid Mechanics

Vol.19,No.1
Mar.,2005

文章编号：1672-9897(2005)01-0011-06

Unsteadiness of shock-wave/boundary-layer interactions induced by unswept and sweptback ramps

HU Cheng-hang, JIANG Wei-min, HUANG Xu-hui, ZHOU Wen-jun, XU Lai-wu
(China Aerodynamics Research & Development Center, Mianyang, 621000, China)

Abstract: The paper presents the results of an experimental investigation on the unsteadiness of shock-wave/boundary layer interactions generated by ten ramps with streamwise angles of 15, 20 and 24 deg. and sweptback angles of 0, 20, 40 and 60 deg. respectively at Mach numbers of 2.011, 2.504 and 3.015. The results show that: (a) The interactions are cylindrical for all unswept and most of the 20 deg. sweptback interactions and quasi-conical for highly sweptback interactions. The decrease of Mach number or the increase of sweptback angle is favorable for the changeover from cylindrical to quasi-conical interaction. (b) The pressure fluctuations in the intermittent region show sharp low-frequency peak. The peak decreases with increasing sweptback or decreasing streamwise angle. However, with the increase of Mach number, the peaks decrease in cylindrical interactions but slightly increase in quasi-conical interactions. The average shock strength is a governing parameter in quasi-conical interaction.

Key words: shock wave/ boundary layer interaction; compression ramp; supersonic flow

后掠与无后掠压缩角模型产生的激波/边界层干扰的非定常特性

胡成行,蒋卫民,黄叙辉,周文军,徐来武
(中国空气动力研究与发展中心,四川 绵阳 621000)

摘要:介绍了 10 个压缩角模型在 M 数为 2.011、2.504、3.015 时产生的激波/边界层干扰的非定常特性的试验研究结果。压缩角模型的流向压缩角分别为 15°、20°、24°,后掠角分别为 0°、20°、40°、60°。实验结果表明:(a)所有无后掠压缩角和大多数 20°后掠压缩角产生柱形干扰,而大后掠压缩角则产生锥形干扰;降低来流 M 数或增大模型后掠角有利于从柱形干扰转变为锥形干扰。(b)间隙区内的压力脉动出现低频峰值,此峰值随着模型后掠角增大或流向压缩角减小而减小;然而随着来流 M 数增大,此峰值在柱形干扰区减小,而在锥形干扰区略增大。对于锥形干扰,无粘激波的平均激波强度是控制其干扰特性的主要因素。

关键词:激波/附面层干扰;压缩角;超声速流
中图分类号:O354.5;V211.753　　**文献标识码**:A

0 Introduction

Shock-wave/boundary-layer interactions (SBI) in supersonic flows are highly unsteady and consequently generate large amplitude fluctuating pressures, which can lead to poor aerodynamic performance and early fatigue, even

* Received date: 2003-11-29; Revised date: 2004-11-29
Author Biography: HU Cheng-hang(1942-), male, Qu county, Sichuan province, researcher. Research field: unsteady aerodynamics.
万方数据

damage of structure. Therefore, the investigation on the unsteadiness of these interactions is of great importance for design of a vehicle and for better understanding of the flow-field physics. Since 1940 's SBI has been the subject of considerable investigations, however, most of the investigations focused attention on the mean-flow behavior of the interaction[1,2]. In contrast, relatively little is known about the unsteadiness of the interaction, though as early as 1950 's S. M. Bogdonoff pointed out that the interaction can be unsteady[3]. Most of the investigations on the unsteadiness of SBI were made in the last decade and their emphases were placed on the separation shock wave structure and space-time correlation of the unsteady signals[4]. The objectives of this investigation are as follows: (a) to determine whether the unsteady properties of these interactions have cylindrical or quasi-conical symmetry, as shown by mean flow measurements. (b) to study the effects of Mach number, streamwise angle and sweptback angle on the interactions.

1 Experimental techniques

The experiments were conducted in a supersonic wind tunnel at Mach numbers of 2.011, 2.504 and 3.015. The tested ramp was mounted on a window of the sidewall of the test section, which was 0.6m wide and 0.6m high. The ramps have streamwise angles (α_s) of 15, 20 and 24 deg. and sweptback angles (λ) of 0, 20, 40 and 60 deg. respectively. To prevent spillage and isolate the interactions from top and bottom wall boundary layers, two fences were attached to the both ends of the unswept ramp, however, only one fence was attached to the apex end of the sweptback ramp (Fig. 1).

Oil flow visualization was used to locate the separation and an array of pressure transducers was used to measure the pressure fluctuations. These transducers were flush mounted in front of the ramp and along three parallel rows, which are perpendicular to the ramp corner and spaced 15 mm between each two rows. The output from a transducer was first filtered and amplified by an amplifier and then digitized and processed by a multi-channel analyzer. All data were filtered at 50 kHz and sampled at 200 kHz/channel. Typically 512k data points per channel were taken. The following quantities and functions were calculated:

万方数据

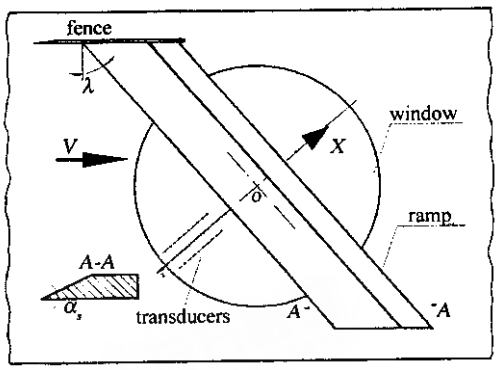

Fig. 1 Sweptback ramp on window
图 1 安装在转窗上的压缩角模型

(1) Pressure fluctuation coefficient, C_p:

$$c_p = \frac{p_{rms}}{q} \times 100\% \tag{1}$$

Where p_{rms} is the root-mean square of pressure fluctuation and q is freestream dynamic pressure.

(2) Non-dimensional power spectrum, G_{nq}:

$$G_{nq} = 10\lg\left(\frac{G(f)}{q^2} \cdot \frac{V}{\delta}\right) \tag{2}$$

Where $G(f)$ is the power spectrum calculated by Fast Fourier Transform method (FFT), V is freestream velocity and δ is undisturbed boundary layer thickness, in the present case $\delta = 38$mm.

(3) Probability density function, PDF:

$$PDF = \frac{N_p}{N} \cdot \frac{1}{\Delta p} \tag{3}$$

Where N is the total data points and N_P is the data points between p_i and $p_i + \Delta p$.

(4) Skewness coefficient, C_s:

$$C_s = \frac{1}{N}\sum_{i=1}^{N}\left(\frac{p_i}{p_{rms}}\right)^3 \tag{4}$$

Kurtosis coefficient, C_k:

$$C_k = \frac{1}{N}\sum_{i=1}^{N}\left(\frac{p_i}{p_{rms}}\right)^4 - 3 \tag{5}$$

Where p_i is the instantaneous pressure fluctuation.

2 Results and discussion

2.1 Results of oil flow visualization

The results of oil flow show that the interactions can be divided into two groups: cylindrical for all unswept and most of the 20 deg. sweptback interactions and quasi-conical for highly sweptback interactions. In cylindrical interactions, the upstream influence and the separation lines

gradually become parallel to the corner line，whereas in quasi-conical interactions these lines appear to emanate from a common point called the virtual conical origin（*VCO*）. The typical oil flow patterns and the classification of the interactions are shown in Fig.2 and in Table 1 respectively.

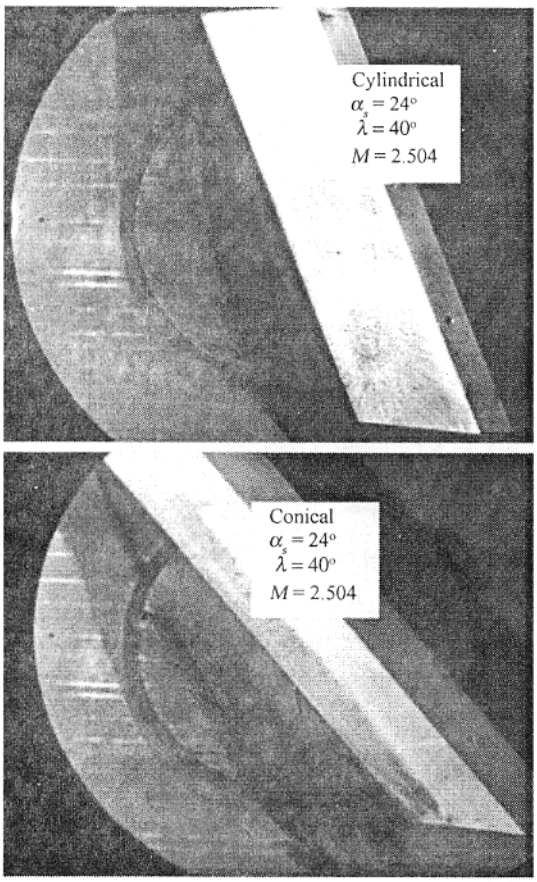

Fig.2　Typical oil flow patterns

图 2　典型油流照片

Table 1　Classification of the interactions

表 1　压缩角模型产生的干扰分类

α_S	M	λ			
		0°	20°	40°	60°
15°	2.011	Cyl.	Cyl.	Con.	Con.
	2.504	Cyl.	Cyl.	Con.	Con.
	3.015	Cyl.	Cyl.	Cyl.	Con.
20°	2.011	Cyl.		Con.	
	2.504	Cyl.		Con.	
	3.015	Cyl.		Con.	
24°	2.011	Cyl.	Con.	Con.	Con.
	2.504	Cyl.	Cyl.	Con.	Con.
	3.015	Cyl.	Cyl.	Con.	Con.

万方数据

2.2　Features of pressure fluctuations

The typical distributions of the pressure fluctuation coefficients（C_p）are shown in Fig.3，plotted in rectangular coordinate（X/δ）for cylindrical interactions and in conical coordinate（θ）for quasi-conical interactions（where X is the vertical distance from a transducer center to the corner line and θ is the swept angle of a ray emanating from the *VCO*）. The locations of the upstream influence and separation are indicated by I and S in the figures. It is illustrated that a sharp pressure fluctuation peak emerges between I and S and then a fairly high plateau

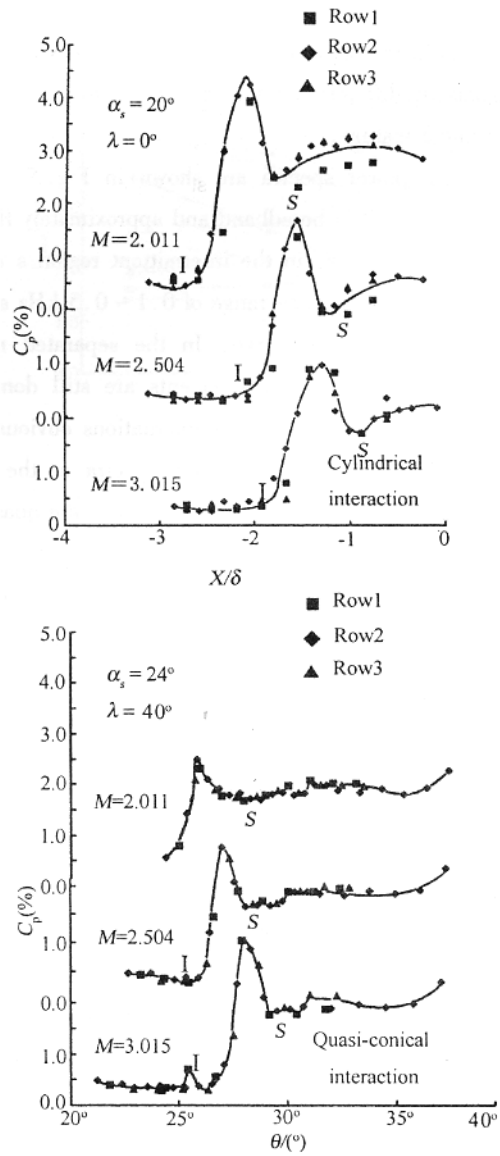

Fig.3　Distributions of pressure fluctuations

图 3　脉动压力分布

level appears in the separated region. The peak is caused by shock oscillation, which induces intermittent separation and reattachment. Therefore, we refer to this region as the intermittent region. Furthermore, the good collapse of data measured in different rows, particularly in the intermittent region, clearly shows that the pressure fluctuation distributions are also cylindrical or quasi-conical symmetry.

Typical time-history plots of the fluctuation signals are shown in Fig. 4. The signals can be divided into three types: (a) wide band, low amplitude fluctuations in the undisturbed flow; (b) low frequency, high amplitude fluctuations in the intermittent region, where "bursting" signals can be clearly seen; (c) high frequency, large amplitude fluctuations in the separated region. The similar natures of the signals at different rows also show a cylindrical or a quasi-conical feature.

Typical power spectra are shown in Fig. 5. In the undisturbed flow it is broadband and approximately flat like white noise. However, in the intermittent region a significant peak in the frequency range of 0.1 ~ 0.5 kHz appears on the power spectrum curve. In the separated region, though the low frequency components are still dominant, the energy of the high frequency fluctuations obviously rises. In addition, the similar power spectra at the corresponding locations indicate the cylindrical or the quasi-conical features in frequency domain.

Fig. 6 shows the typical probability density functions (PDF) of the pressure fluctuation signals. In general, the PDFs are essentially Gaussian in the undisturbed or separated region. However, in the intermittent region, especially when the maximum fluctuation occurs, the PDFs are obviously skewed. Moreover, the PDF in cylindrical interaction presents a bimodal curve similar to the PDF of a sine signal with random noise. This suggests that the fluctuations have random low amplitude, high frequency fluctuations superposed on qusi-periodic high amptitude, low frequency fluctuations. The PDF in the quasi-conical interaction, though skewed, has only one peak. This indicates that the fluctuations in quasi-conical interactions are more random than those in cylindrical interactions. Fig. 7 gives the skewness coefficient (C_s) and kurtosis coefficient (C_k) which indicate the degrees of symmetry and steepness of the

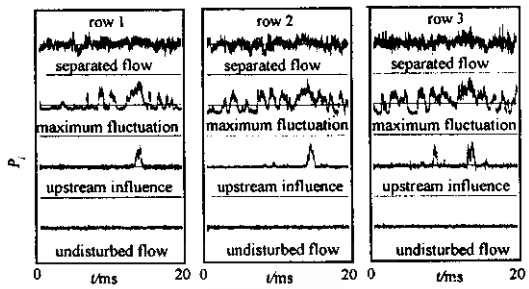

Fig. 4 Time-history plots of pressure fluctuations
图 4 脉动压力信号的时间历程

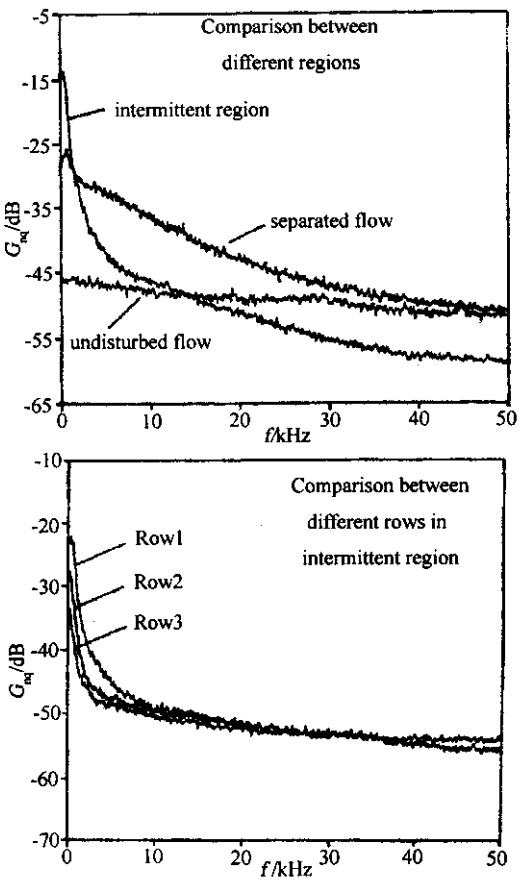

Fig. 5 Non-dimensional power spectra
图 5 脉动压力无量纲功率谱密度

PDF curve respectively. For Gaussian distribution, both C_s and C_k are equal to zero. It can be seen that C_s and C_k in undisturbed and separated regions approximate to zero, proving the PDFs in these regions to be Gaussian. However in the intermittent region C_s and C_k vary sharply, indicating that the flow in this region is most unsteady.

万方数据

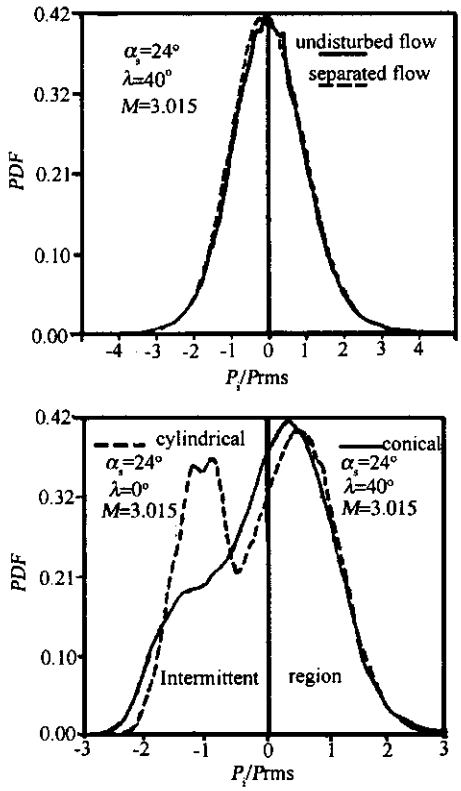

Fig.6 Probability density functions of pressure fluctuations

图 6 脉动压力的概率密度函数

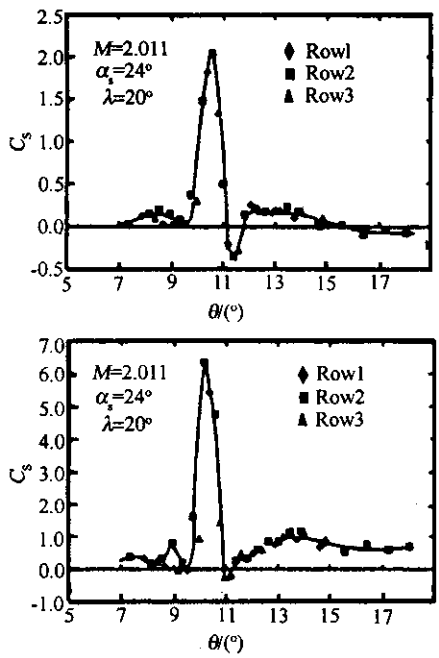

Fig.7 Distributions of skewness (C_s) and kurtosis (C_k)

万劈数据度系数 C_s 和峰态系数 C_k 分布

2.3 Effects of Mach number, streamwise and sweptback angle of the ramp on the interaction

With increase of Mach number, the maximum pressure fluctuations decrease in cylindrical interactions, but slightly increase in quasi-conical interactions (Fig. 8). With decrease of streamwise angle or increase of sweptback angle, the pressure fluctuations decrease in both cylindrical and quasi-conical interactions (Fig. 8). The decrease of Mach number or the increase of sweptback angle is favorable for the changeover from cylindrical to quasi-conical interaction (Table 1).

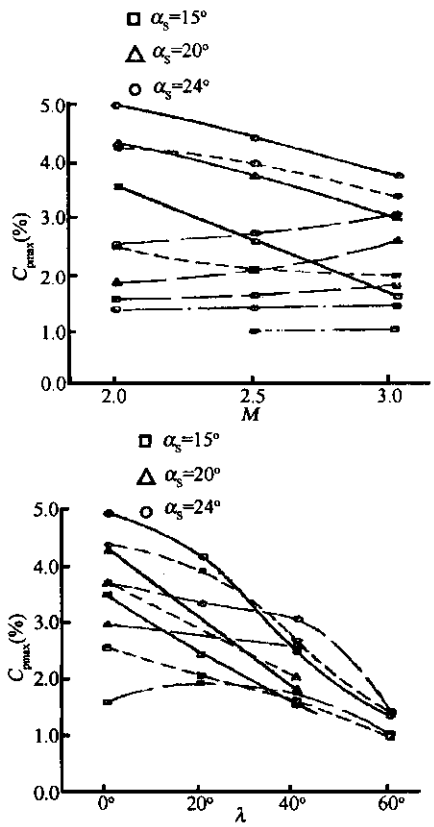

Fig.8 Variation of $C_{p\ max}$ with Mach number and sweptback andgle

图 8 $C_{p\ max}$ 随 M 数和后掠角的变化

Prof. Deng's investigation showned that the mean features in the quasi-conical interaction are mainly governed by the average shock strength, (Mn)[5,6]. The present investigation further shows that the unsteadiness of quasi-conical interactions are also governed by Mn, as shown in Fig. 9, where $(P_{rms}/p_\infty)_{max}$ can be well correlated by Mn. However, the data in cylindrical interactions, though processed in the same way, can not collapse on a

single curve. This suggests that cylindrical interactions are far more complex than quasi-conical interactions.

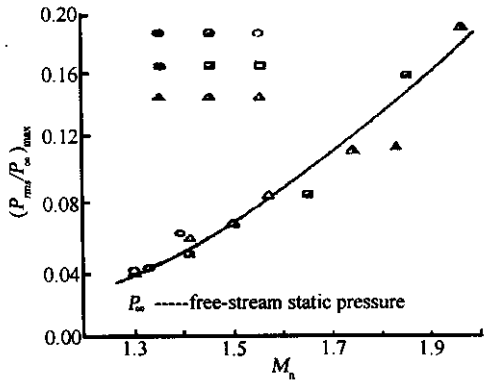

Fig.9 Effect of average shock strength on quasi-conical interaction

图 9 平均激波强度对锥形干扰的影响

3 Conclusions

(1) The oil flow patterns show that the interactions induced by all unswept and most of the 20 deg. sweptback ramps are cylindrically symmetric, whereas those generated by highly sweptback ramps are quasi-conically symmetric. Furthermore, the unsteadiness in the interaction region also appears cylindrically or quasi-conically symmetric respectively. The decrease of Mach number or the increase of sweptback angle is favorable for the changeover from cylindrical to quasi-conical interaction;

(2) The pressure fluctuations in the intermittent region show a high peak, generated by the oscillating shock wave and dominated by low-frequency fluctuations of 0.1 to 0.5 kHz. The peak decreases with increasing sweptback angle or decreasing streamwise angle. With the increase of Mach number, the peak decreases in cylindrical interactions but slightly increases in quasi-conical interactions. The features (both steady and unsteady) of quasi-conical interaction are mainly governed by the average shock strength (Mn). However, cylindrical interactions are far more complex than quasi-conical interactions.

Acknowledgments: The authors would like to thank prof. Deng Xue-ying of Beijing University of Aeronautics and Astronautics for his helpful technical suggestions.

参考文献:

[1] SETTLES G S, DOLLING D S. Swept shock/boundary-layer interactions [R]. A1AA Paper 90-0375, 1990.

[2] SETTLES G S, DOLLING D S. Swept shock-wave/boundary-layer interactions, Tactical missile aerodynamics: General topics [M]. Chapter 12, Published by the American Institute of Aeronautics and Astronautics, Inc. 1992.

[3] BOGDONOFF S M. Some experimental studies of the separation of supersonic turbulent boundary layers [R]. Rept 336, Aero. Eng. Dept., Princeton Univ., 1955.

[4] DOLLING D S. Unsteadiness of shock wave-induced turbulent boundary layer separation-A review [R]. Proceedings of the IUTAM symposium on turbulent shear-layer/shock-wave interactions, edited by J. Delery, Palaiseau, France, 1986.

[5] DENG Xue-ying, LAO Jin-hua. ZHANG Hua. Improvement of conical similarity rule in swept shock wave/boundary layer interaction [R]. A1AA 93-2941, 1993.

[6] LAO Jing-hua, DENG Xue-ying. A simple similarity law of conical shock wave [R]. A1AA 94-2308, 1994.

万方数据